



Research article

Reservoir sands characterisation involving capacity prediction in N_Z oil and gas field, offshore Niger Delta, Nigeria

Anthony I Nzekwu¹ and Richardson M Abraham-A^{2,*}

¹ Department of Applied Geophysics, Federal University of Technology, Akure (FUTA), Ondo State, Nigeria

² Institute of Energy and Environment, University of São Paulo (IEE-USP), São Paulo, Brazil

* **Correspondence:** Email: abrahamrichardson@usp.br; Tel: +5511989198067.

Abstract: Hydrocarbon exploration is a high-risk venture; therefore, pre-determining reservoirs' capacities is pertinent, reducing associated uncertainties regarding hydrocarbon presence and production. This study delineates hydrocarbon-bearing sands, determines the reservoir area extent, computes the associated petrophysical parameters and presents the reserve volume estimation based on wireline logs with integrated 3-D seismic surveys. It evaluates and indicates three (3) hydrocarbon-bearing reservoirs sands ($N_{Z(R1)}$, $N_{Z(R2)}$ and $N_{Z(R3)}$) of varying thicknesses (h) across three (3) wells reservoirs $N_{Z(R1)}$, $N_{Z(R2)}$ and $N_{Z(R3)}$. The reservoir properties, including porosity (Φ), free fluid index (FFI), permeability (K), fluid saturations and reservoir thickness (h), represent potentially viable hydrocarbon reservoir units across the field. It presents the estimation of the recovery factor based on the FFI values. Across the reservoirs, Φ is 0.28 in $N_{Z(R1)}$, 0.27 in $N_{Z(R2)}$ and 0.26 in $N_{Z(R3)}$. FFI is 0.26 in $N_{Z(R1)}$, 0.25 in $N_{Z(R2)}$ and 0.26 in $N_{Z(R3)}$. K is 10388 mD in $N_{Z(R1)}$, 8304mD in $N_{Z(R2)}$, and 6580 mD in $N_{Z(R3)}$. Water saturation (S_w) is up to 0.4, 0.36 and 0.20 with the associated hydrocarbon saturation (S_h) of 0.60, 0.64 and 0.80 corresponding to $N_{Z(R1)}$, $N_{Z(R2)}$ and $N_{Z(R3)}$. Considering the delineated reservoir areas based on the prevailing fault assisted structural style, the total volume of recoverable oil is 11.3×10^6 , while the gas capacity is 1.8×10^9 cuft. These findings will aid the field's oil and gas reservoir developmental activities and serve as reference points to related studies involving similar objectives.

Keywords: capacity estimation; moveable fluid; porosity; permeability; sandstone reservoir; free fluid index; recovery factor

1. Introduction

Hydrocarbon exploration activities, usually, are capital intensive. Therefore, predicting the in-situ hydrocarbons reserves and recoverable volumes of oil and gas from a targeted hydrocarbon reservoir is pertinent to proper production plans. The role of geophysics in the oil and gas industry is immense and indispensable amongst the ranges of oil and gas exploration and exploitation technologies. Previous works [1–8] involving hydrocarbon exploration or closely related findings have showcased the relevance of petrophysics and seismic models in geophysical or geological investigations.

Therefore, this study delineates hydrocarbon traps and predicts the associated reservoir volumes in the N_Z Oil and Gas field, offshore Niger Delta, based on petrophysics and seismic models. It aims to indicate the percentage of the movable fluid, aiding to predict the reservoirs' hydrocarbon recovery factor (RF). It also involves fluid contact delineations to show the presence of gas and oil and inform the possibilities of concerning associated water production. Proliferous source rocks involving deeply buried sediments, which can convert their original organic matter into hydrocarbons, are indispensable concerning oil and gas formation. Oil and gas accumulation depends on the associated hydrocarbon source rock viability and other geological parameters in commercial quantities. Porosity (Φ) networks, permeability (K), relative fluid permeability, fluid viscosity, suitable trap configuration, considerable depths of burial, amongst others [9–12], are pertinent to hydrocarbon availability and recoverability within geological reservoirs. According to Wang Qin [13], a geologic trap consists of combined rock structures that harbour hydrocarbon and prevent oil and gas lateral or vertical mobility. A stratigraphic trap consists of unconformity, reef or a pinch out, while structural consists of folded or faulted units; therefore, either or both may form the fluid (gas, oil and water) trap [14]. Thus, this study defines the trap types associated with the N_Z oil and gas field to predict the volumes of hydrocarbons in place adequately and to minimise uncertainties concerning resource presence with underestimation or exaggeration of reservoir capacities.

Reservoir's parameters, including porosity, permeability, fluid saturation, recovery factor and oil volume factor, are essential inputs in reserve estimation [15–17]. Reserves include estimated recoverable quantities of oil and gas from established accumulations and may be classified based on the degree of certainty as proven, probable and possible [18]. Knowledge of reservoir dimensions such as the thickness and area extent is essential in reservoir volumetric analysis. The volumetric estimation of hydrocarbons is required early to plan development activities, such as the long-term drilling sequence, platforms, pipelines, processing facilities [19]. In addition, the synthetic seismogram, which is the link between particular lines of strata, defined in depths, and the seismic expression of that sequence defined in time [20] is generated from the good logs of the field in question and incorporated into the interpretation procedure to enhance better resolution work. Therefore, this research seeks to integrate 3-D seismic surveys with well log data to reveal subsurface geological structures responsible for oil and gas accumulation. It also looks forward to estimating the recoverable hydrocarbon in reservoirs $N_{Z(R1)}$, $N_{Z(R2)}$ and $N_{Z(R3)}$ delineated across wells $N_{Z(W1)}$, $N_{Z(W2)}$ and $N_{Z(W3)}$ in the N_Z oil and gas field within Niger Delta.

2. Study location and petroleum geology

N_Z oil and gas field falls within the offshore continental margin of the Niger Delta, enclosed by the latitude of 5.3 °N and 5.4 °N and longitude 5.9 °E to 6.0 °E (Figure 1). The three (3) wells, $N_{Z(W1)}$, $N_{Z(W2)}$ and $N_{Z(W3)}$, are within the study area, and the seismic survey comprises 41 inlines and 23 crosslines. The study location forms part of the hydrocarbon-rich provinces within the southwest of Nigeria's geological formations consisting of sedimentary rocks associated with a series of the Delta's developmental events.

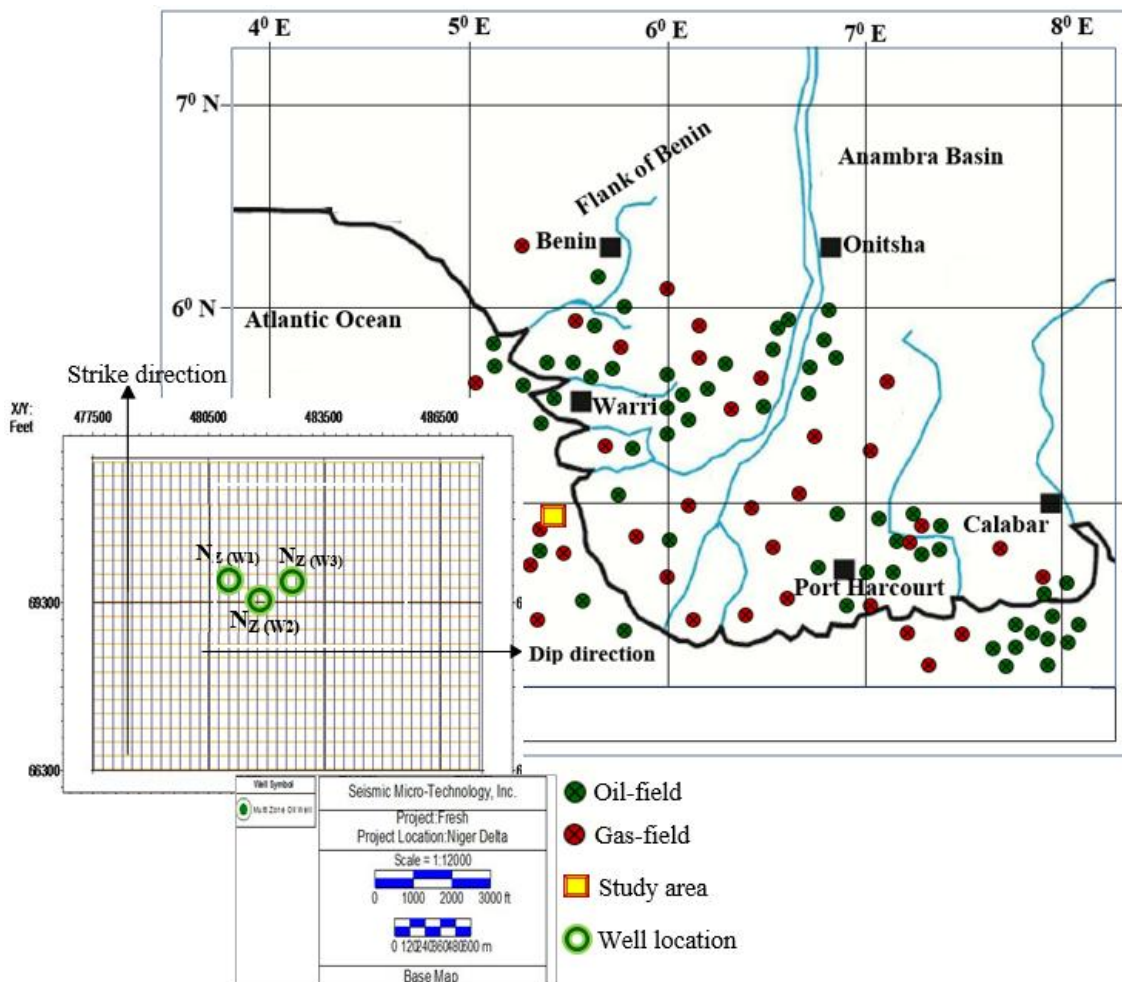


Figure 1. Niger Delta hydrocarbon field and the index map, showing strike/deep lines representing the study location. Modified from Abraham-A and Taoli [10].

The development extended from Eocene to Mid-Miocene sub-deltas to the growth of the post-Mid-Miocene Delta. Niger Delta complex progressed along existing sedimentary axes from the Eocene to the Mid-Miocene. The axes include the Anambra and its subsidiary basins, fed by the Niger and Benue River, and the Afikpo syncline fed by the Cross River, which deposited some materials during the Eocene to Late Oligocene [21]. After the mid-Miocene, the Niger-Benue and Cross River Delta systems merged. From then, the rate of delta advances was determined by the erosion rate of newly uplifted blocks in the hinterland, particularly of newly emergent ones in Cameroon Mountain [21,22]. The Niger Delta consists of three (3) sedimentary depositional

successions; Benin, Agbada and Akata Formations. The associated rocks are mainly interlayered shale and sandstone beds across the three (3) geologic units. The Benin Formation consists of coarse-grained, locally fine-grained, poorly sorted, subangular to well-rounded sandstones [23]. It has thicknesses ranging from 0.2–100 m, and the sand and sandstone are coarse to fine and commonly granular in texture. Very little hydrocarbon accumulation is associated with this highly porous and generally freshwater-bearing Benin Formation [22].

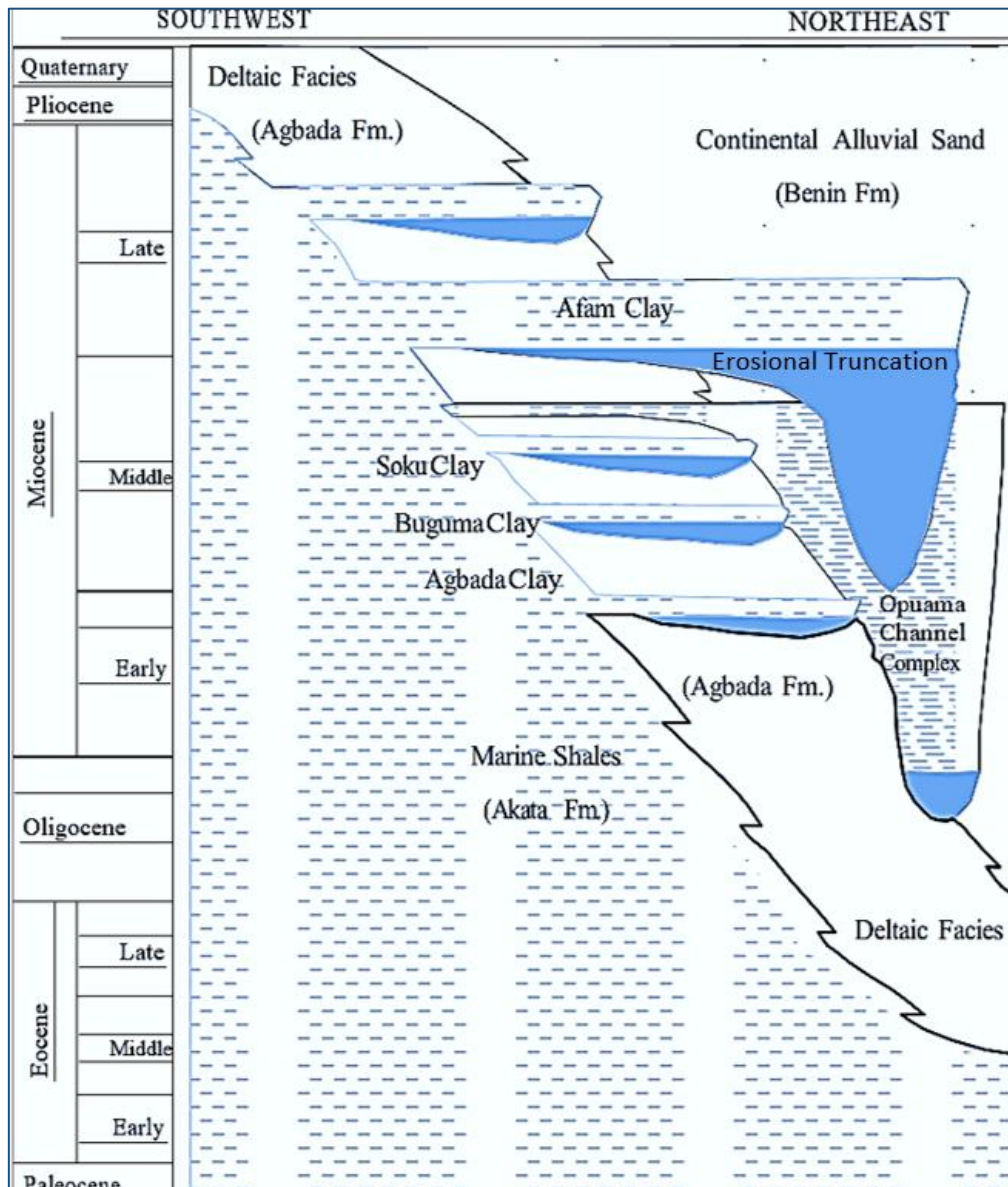


Figure 2. Stratigraphic successions of the Niger Delta. Modified from Doust and Omatsola [24].

The Agbada Formation consists of paralic, mainly shelf deposits of alternating sands and shales. The sandy parts serve as the main hydrocarbon reservoir of the Delta and shale as the caprock. The sequence is associated with synsedimentary growth faulting and is thickest at the centre of the Delta, up to 457.2 m. The upper part is a predominantly sandy unit with minor shale intercalation, and a lower shaly layer is thicker than the sandy upper unit [24–27]. Therefore, the depositional environment is transitional, between the upper continental Benin Formation and the Marine underlying Akata

Formation. Akata formation, the deepest stratigraphic unit, is chiefly represented by plastic, low density, under-compacted and high-pressure shallow marine to deep water-shale; with only local inter-beddings of sands and siltstones. In general, the shale is over-pressured, providing the mobile base for subsequent growth faulting associated with the deposition of the overlying paralic sequence. There are several presentations on the source of the Niger Delta; some believe the Agbada Formation as the source rock, others present the Agbada source, and some others present the combined Agabda and Akata source [22,23,25,27–30]. According to Doust and Omatsola [24], the shale of both the paralic and open marine sequences of the Agbada and Akata Formations are most likely the widely disseminated source rock in the Niger Delta considering the organic matter content.

The ability of the reservoir units to trap and accumulate hydrocarbons over time within the Niger Delta is significant, encouraging the immense exploration known with the region. Structures, such as growth faults, rollover anticlines, and rock diapirs, define the prevailing hydrocarbon traps in the Niger Delta Basin. Combined fault systems are the dominant structural features in the Niger Delta [7,31,32]. The continental breakup with the African and South American plates rifting resulted in the associated structural style of the Delta structures [33–37]. The associated rifting in the Delta commenced from the Late Jurassic to Late Cretaceous. Gravity influenced tectonism emerged as a significant force, controlling other structural deformations and contributing to the prevailing structural style aiding the migration, accumulation and production of hydrocarbons within the prolific zones [34,38–41].

3. Materials and methods

Petrophysical data consisting of gamma-ray (GR), neutron (NPHI), density (RHOB), water saturation (S_w), and deep induction (ILD) with incorporated 3-D seismic data were engaged. While GR and ILD aided to distinguish potential hydrocarbon-bearing reservoir sands from shale, NPHI and RHOB aided fluid differentiation. Other qualitative evaluations include the determination of porosity (Φ), free fluid index (FFI), permeability (K), volume of shale (V_{sh}), hydrocarbon saturation (S_h), water saturation (S_w) and reservoir thickness (h). The seismic interpretation includes horizons and faults mappings, time-depth and conversion using the check-shot survey data, delineation of the hydrocarbon zone with the reservoir area based on the structure map. Therefore, hydrocarbons in place and recoverable volumes were estimated using appropriate equations.

The study evaluates and presents qualitative and quantitative parameters. The fundamental parameter estimated from the wireline log and relevant expression is Φ . The density-derived porosity (Φ_D) corrected for shale based on Equation (1) was engaged.

$$\Phi_D = \frac{\rho_{ma} - \rho_b}{\rho_{ma} - \rho_f} - V_{sh} \left[\frac{\rho_{ma} - \rho_{sh}}{\rho_{ma} - \rho_f} \right] \quad (1)$$

Where; V_{sh} is the volume of shale in the form of Equation (2)

$$V_{sh} = 0.83(2^{(3.7 \times IGR)} - 1.0) \quad (2)$$

ρ_{ma} = matrix density of formation (2.65g/cc for sandstone), ρ_b = bulk density of the formation; ρ_f = fluid density of formation (1.0gm/cc) and ρ_{sh} = bulk density of adjacent shale.

Free fluid index (FFI) defines the moveable fluid within the reservoir. Equation (3) is the FFI expression redefined by Abraham-A and Taoili [11] for sandstone, based on Schlumberger [42]. The expression follows a sensitivity analysis to verify the effects of the variation in the values of tortuosity factor (α) and cementation exponent (m) on the irreducible water saturation (S_{wirr}) within sandstone reservoirs.

$$FFI = \Phi - 0.02 \quad (3)$$

Permeability (K) takes the form of Equation (4), also redefined for sandstone by Abraham-A and Taoili [11], considering FFI and Coates and Denoo [43] expression.

$$K = 10^4 \Phi^4 \frac{(\Phi - 0.02)^2}{0.0004} \quad (4)$$

Oil in place (OIP) and gas in place (GIP) take the form of Equations (5 and 6) [17].

$$OIP = Cc A_d h \Phi (1 - S_w) \text{bbl} \quad (5)$$

$$GIP = Cc A_d h \Phi (1 - S_w) \text{Cu. ft.} \quad (6)$$

Cc = conversion constant (7758 converts' oil volume from acres to bbl and 43560 converts' gas volume acres to cubic feet) [15, 44];

Recoverable volumes of oil and gas (V_{Ro} and V_{Rg}) take the form of Equations (7 and 8);

$$V_{Ro} = \frac{OIP}{FVF} \times R.F \quad (7)$$

$$(V_{Rg}) = \frac{GIP}{FVF} \times R.f \times \frac{P_{f_2}}{P_{f_1}} \quad (8)$$

Such that, FVF is the formation volume factor expressed as Equation (9):

$$FVF = 1.05 + 0.5 \times \frac{GOR}{100} \quad (9)$$

R.F = recovery factor and GOR = gas to oil ratio and

$$\frac{P_{f_2}}{P_{f_1}} = \frac{0.43 \times \text{depth}}{15} \quad (10)$$

(P_{f_2} = Reservoir pressure, P_{f_1} = surface Pressure (15 atm) and 0.43 = universal average pressure gradient, and depth corresponding to the gas top).

4. Results

The research identifies lithologic units, delineates reservoirs, predicts fluid types, interprets seismic structural maps, and estimates reservoir volume based on geophysical (seismic and petrophysical) models. Three (3) hydrocarbon-bearing reservoirs, $N_{Z(R1)}$, $N_{Z(R2)}$ and $N_{Z(R3)}$, were correlated across wells $N_{Z(W1)}$, $N_{Z(W2)}$ and $N_{Z(W3)}$ (Figure 3). Fluid type's identification aided by the combined NPHI and RHOB signatures reveals gas-oil and oil-water interfaces, confirming gas-oil-water-bearing in $N_{Z(R2)}$ across $N_{Z(W2)}$. A significant separation between the density and neutron porosity signatures within the hydrocarbon-bearing zone indicates gas presence (Figure 4).

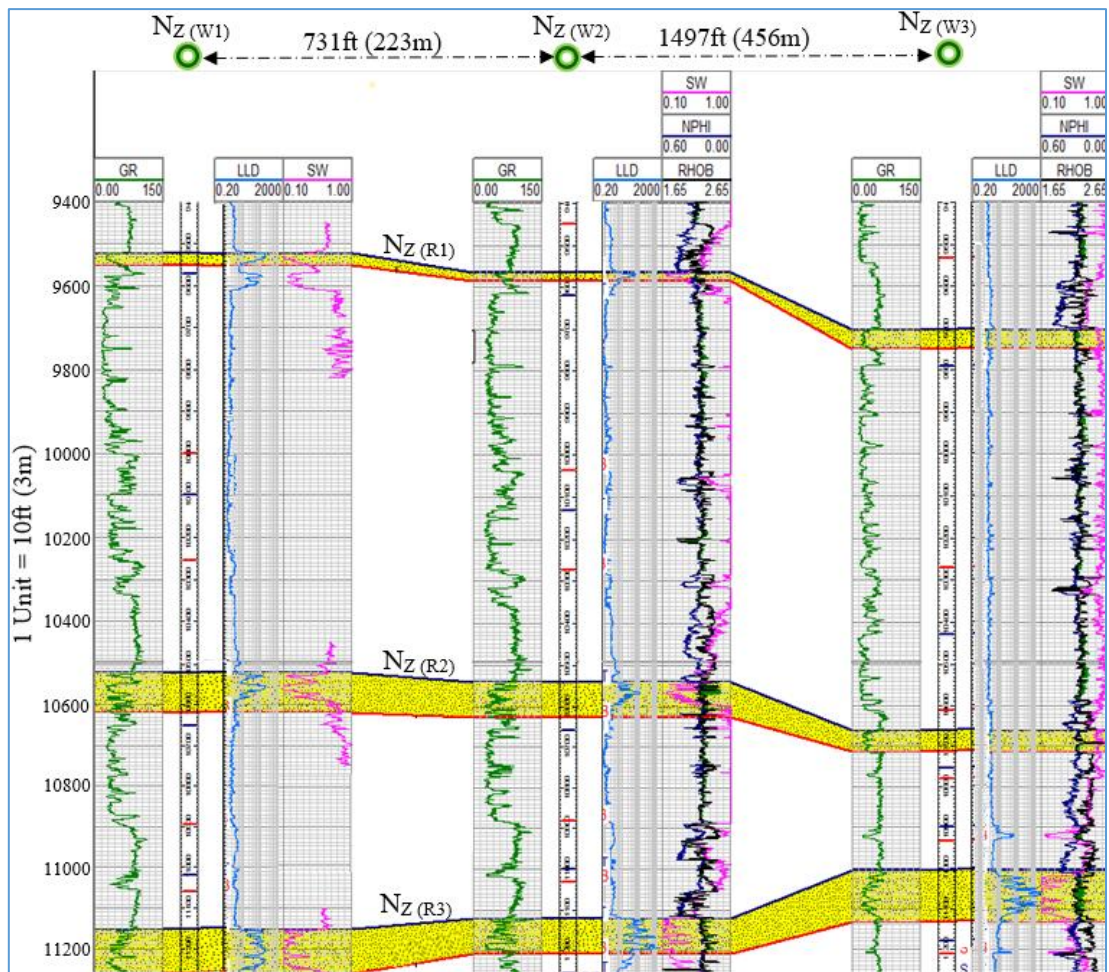


Figure 3. $N_{Z(R1)}$, $N_{Z(R2)}$ and $N_{Z(R3)}$ correlation across $N_{Z(W1)}$, $N_{Z(W2)}$ and $N_{Z(W3)}$.

Three (3) consecutive horizons (Figure 5), representing the tops of $N_{Z(R1)}$, $N_{Z(R2)}$ and $N_{Z(R3)}$ across $N_{Z(W1)}$, $N_{Z(W2)}$ and $N_{Z(W3)}$, were mapped. The horizons encountered associated tectonic faulting across the field considering two-way travel time (TWT) intervals between 2.40 and 2.90 seconds. The combination of the fault sets exemplifies a similar trend of structural closures with potentials for hydrocarbon trapping.

One of the wells, $N_{Z(W2)}$, has a sonic log and was combined with density logs to generate a synthetic seismogram (Figure 6), aiding to tie seismic to well data and check the quality of the reflection event on the seismic section. It is observable that the top of the different sand units within coincided with the respective seismic horizon representing $N_{Z(R1)}$, $N_{Z(R2)}$, and $N_{Z(R3)}$ in times and depths.

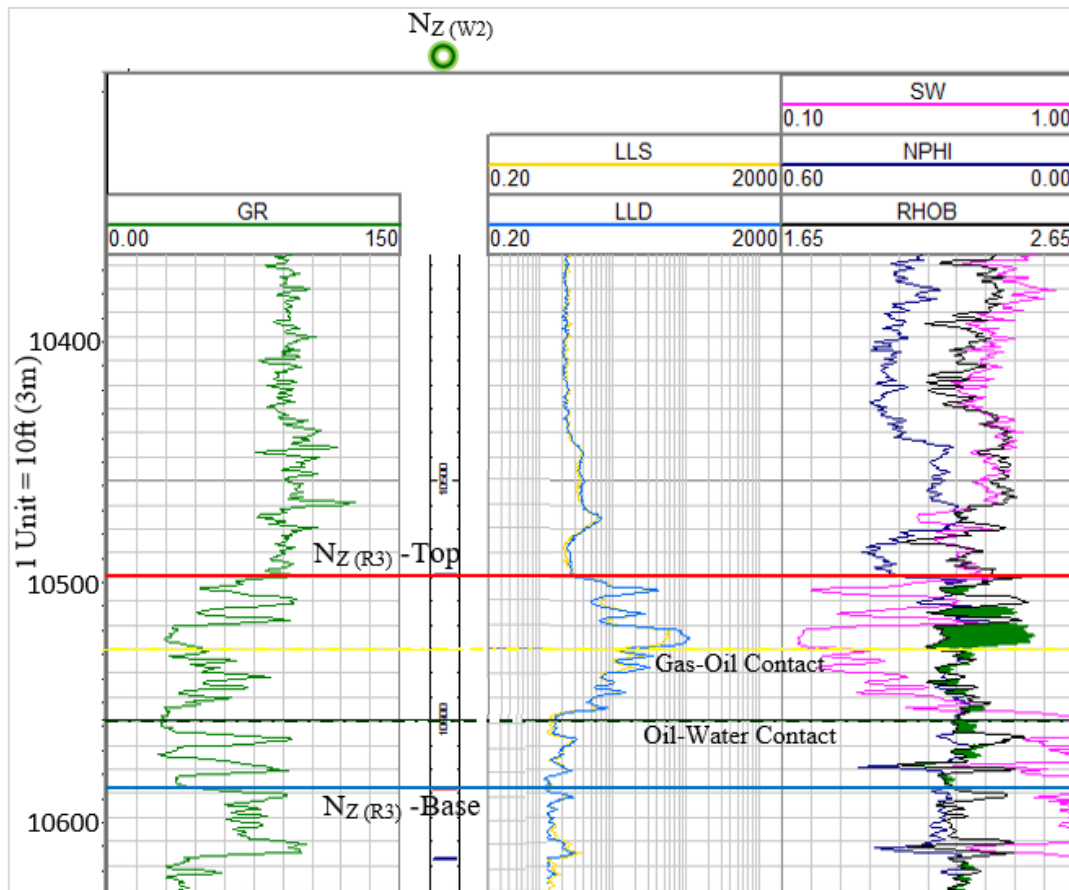


Figure 4. Fluid contacts within $N_{Z(R2)}$ across $N_{Z(W2)}$.

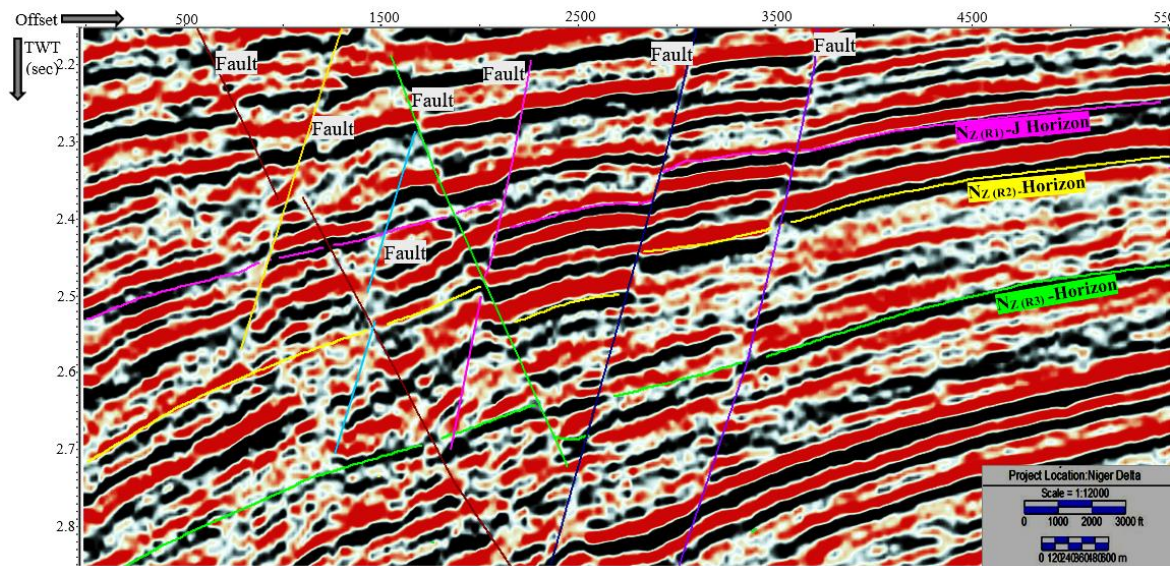


Figure 5. Typical inline seismic section showing the selected fault planes and reservoir horizons.

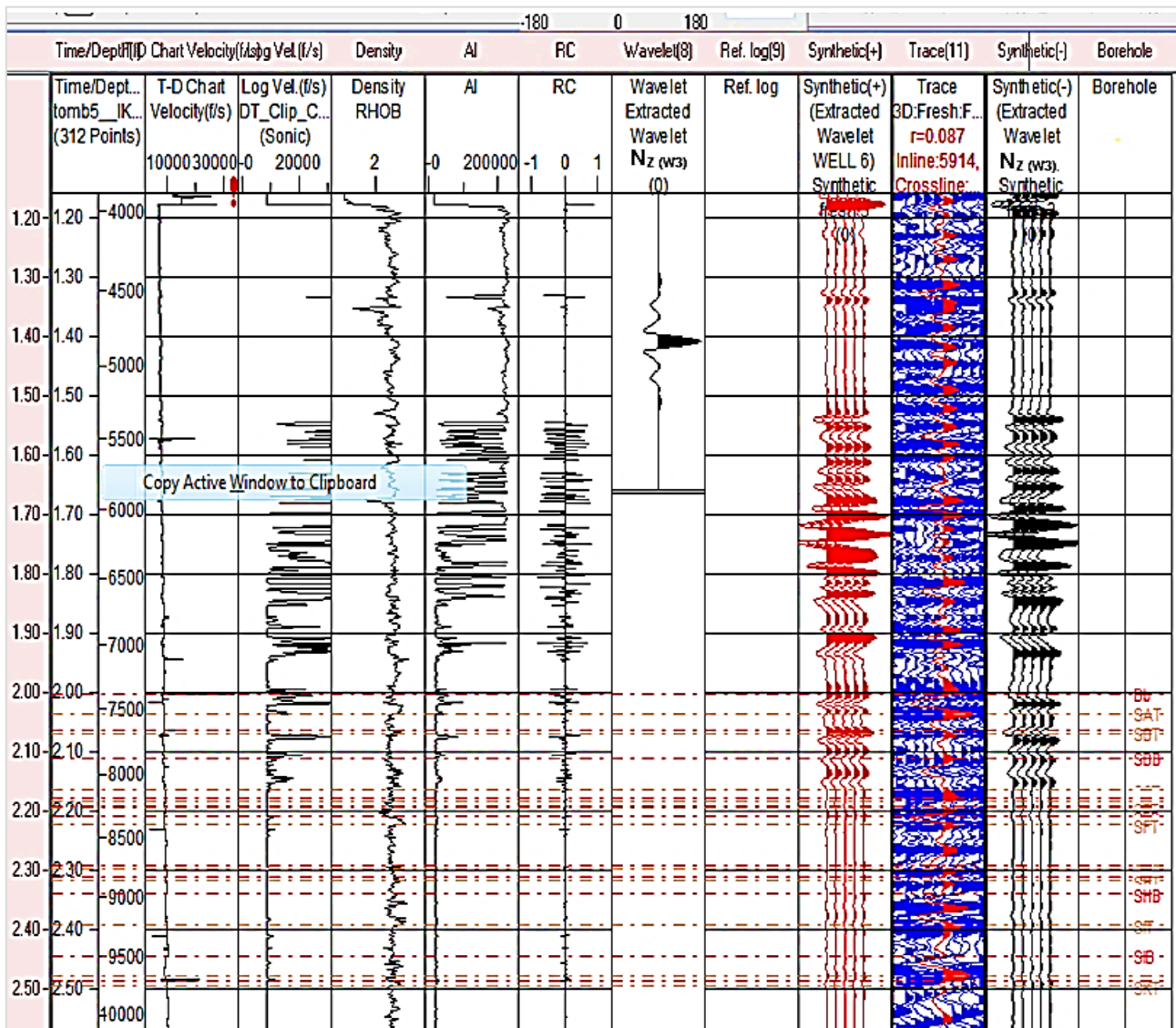


Figure 6. Synthetic seismogram indicating seismic to well logs ties.

Figure 7 shows the depth structure maps representing the selected seismic horizons. $N_{Z(R1)}$ -Horizon tracks between 2.096 s and 2.668 s TWT and 7759 ft. (2365 m) and 10589ft (32278 m). $N_{Z(R2)}$ -Horizon tracks between TWT of 2.217 s and 2.978 s, and 8322 ft. (2537 m) and 12031ft (3667 m). Similarly, $N_{Z(R3)}$ -Horizon tracks between 2.309 s and 3.101 s TWT and 12930 ft. (3941 m) and 8815 ft. (2687 m). The structure maps reveal that $N_{Z(R1)}$ is composed of oil and water with an oil zone of about 131 acres. $N_{Z(R2)}$ comprises a gas layer covering approximately 112 acres and an oil layer of about 177 acres. Furthermore, $N_{Z(R3)}$ has an oil layer covering a total area of 152 acres with a water layer beneath.

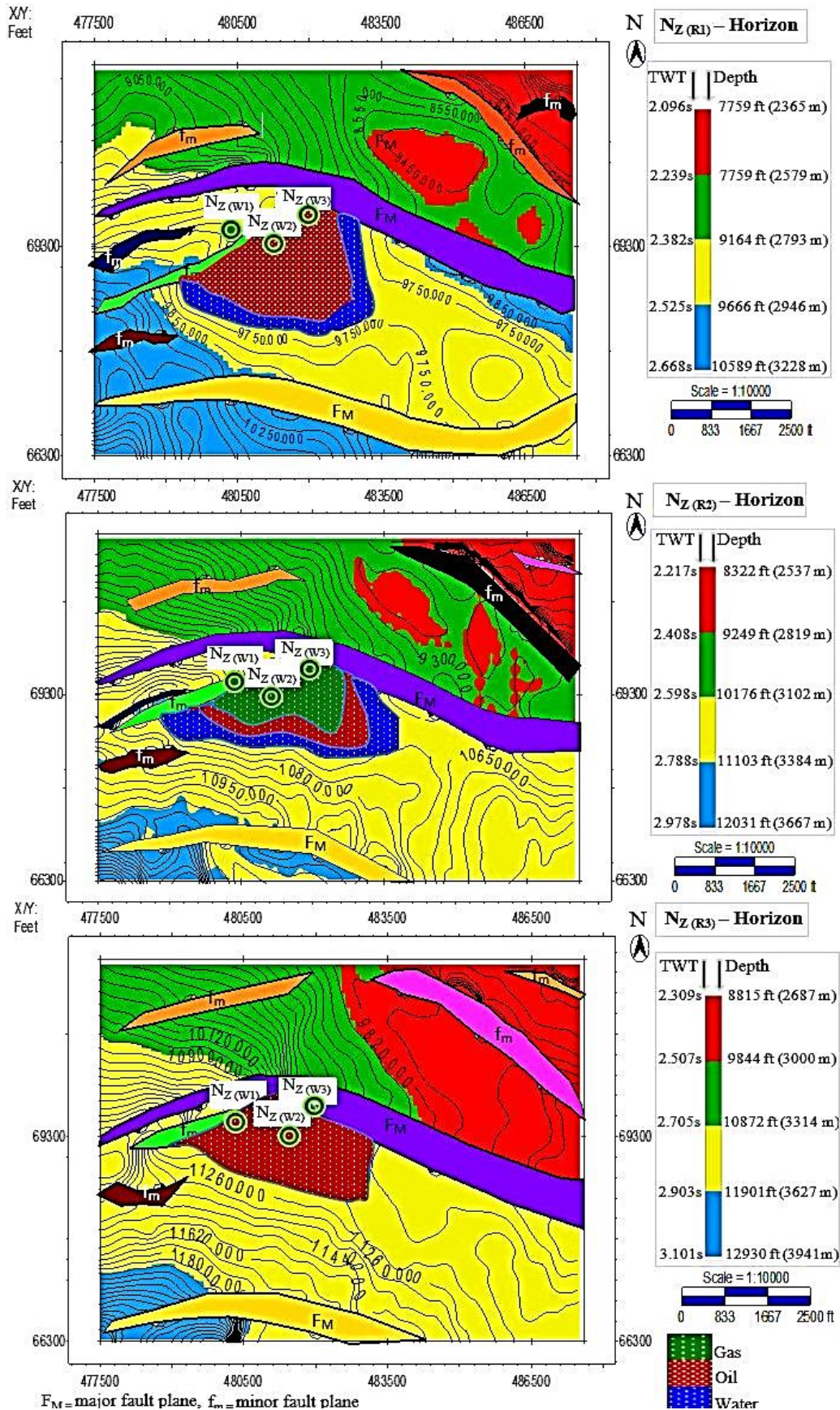


Figure 7. Structure maps indication trap type, hydrocarbon presence and fluids contacts.

Table 1 presents the average values obtained based on the petrophysical and volumetric estimations. $N_{Z(R1)}$, $N_{Z(R2)}$ and $N_{Z(R3)}$ across $N_{Z(W1)}$, $N_{Z(W2)}$ and $N_{Z(W3)}$. The average value for FFI is approximately 0.25, and K values are also significantly high. FFI indicate the moveable fluid within the reservoirs [11,42]; therefore, a recovery factor of 25% is adopted in the volumetric expression to compute the recoverable volumes of gas and oil.

Table1. Qualitative and quantitative estimates based on the reservoirs.

Parameters	$N_{Z(R1)}$	$N_{Z(R2)}$	$N_{Z(R3)}$
The volume of shale (V_{sh})	0.059	0.029	0.111
Porosity (ϕ)	0.28	0.27	0.26
Free fluid index (FFI)	0.26	0.25	0.24
Permeability(K)	10388 mD	8304 mD	6580 mD
Oil thickness (h)	28 ft. (8.5 m)	62 ft. (18.9 m)	115 ft. (35.1 m)
Gas thickness (h)	–	30 ft. (9.1 m)	–
Water saturation S_w	0.40	0.36	0.20
hydrocarbon saturation S_h	0.60	0.64	0.80
Drainage area oil (acres)	131 acres	177 acres	152 acres
Drainage area gas (acres)	–	112 acres	–
oil in place (IOP)	4,780,666 bbl	14,711,551 bbl	28,206,847 bbl
Recoverable oil reserve	1,129,113 bbl	3,474,622 bbl	6,661,986 bbl
gas in place (GIP)	–	25, 291,285 cu.ft.	–
Recoverable gas reserve	–	1,797,986,922 cu.ft	–

5. Discussion

The evaluation includes the correlation of three (3) reservoirs designated $N_{Z(R1)}$, $N_{Z(R2)}$ and $N_{Z(R3)}$ across wells $N_{Z(W1)}$, $N_{Z(W2)}$ and $N_{Z(W3)}$. The three (3) wells are located within the depth of the Agbada Formation stratigraphic column. The reservoir correlation panel shows that $N_{Z(W1)}$ penetrates $N_{Z(R1)}$ at 9520 ft (2901.696 m), $N_{Z(R2)}$ at 10520 ft (3206.496 m), and $N_{Z(R3)}$ at 11150 ft (3398.52 m). $N_{Z(W2)}$ reaches $N_{Z(R1)}$ at 9560 ft (2913.888 m), $N_{Z(R2)}$ at 10540 ft (3212.592 m), and $N_{Z(R3)}$ at 11120 ft (3389.376 m). Furthermore, $N_{Z(W3)}$ encounters $N_{Z(R1)}$ at 9700 ft (2956.56 m), $N_{Z(R2)}$ at 10660 ft (3249.168 m), and $N_{Z(R3)}$ at 10000 ft (3048 m). The sandstone reservoirs occur consistently interbedded with shale units described as the hydrocarbon source rocks of the Niger Delta. The synthetic seismograph confirmed that the $N_{Z(R1)}$, $N_{Z(R2)}$ and $N_{Z(R3)}$ tied in times and depths considering the wireline log information and seismic reservoir horizon. $N_{Z(R1)}$ -Horizon tracks between 2.096 s and 2.668 s, $N_{Z(R2)}$ -Horizon occurs between 2.217 s and 2.978 s, while $N_{Z(R3)}$ -Horizon is between 2.309 s and 3.101s two-wat travel time (TWT).

The average volume of shale is 0.059 (5.9%) in $N_{Z(R1)}$, 0.026 (2.6%) in $N_{Z(R2)}$ and 0.113 (11.3%) in $N_{Z(R3)}$, indicating relatively clean or reasonably shale free sandstone units. $N_{Z(R1)}$ has an average porosity (Φ) of 0.28 (28%), free fluid index (FFI) of 0.26 (26%), permeability (K) of 10388 mD, and hydrocarbon saturation (S_h) of 0.6 (60%) with the corresponding water saturation (S_w) of 0.4 (40%). For $N_{Z(R2)}$, (Φ) is 0.27 (27%), FFI is 0.25 (25%), K is 8304 mD, S_h is 0.64 (64%), and S_w is 0.36 (36%). Also, for $N_{Z(R3)}$, Φ is 0.26 (26%), FFI is 0.24 (24%), K is 6580 mD, S_h is 0.8 (80%), and S_w is

0.36 (36%). $N_{Z(R1)}$ has an average thickness (h) of 28 ft. (8.5 m), $N_{Z(R2)}$ is 62 ft. (18.9 m), and $N_{Z(R3)}$ is 115 ft. (35.1 m). Further differentiation of hydrocarbons contacts using a combination of the bulk density (RHOB) and neutron (NPHI) logs reveals a 30 ft. (9.1 m) thick gas layer at 10500 ft. (3200.4 m) in $N_{Z(W2)}$.

Eight (8) fault planes were identified and mapped in the study area. While F_M represents growth (major) faults, cutting across the entire N_Z oil and gas field, f_m denotes minor fault planes which tend to disappear after some distance across the area. Some fault sets are synthetic, trending east-west, and dip southerly, while others are antithetic and in the northern direction. The fault set's orientation and combination aided in identifying structural highs and fault-dependent closures. $N_{Z(R1)}$ has an estimated drainage area of 131 acres with oil in place (OIP) of 4,780,666 bbl and a corresponding recoverable oil volume (V_{RO}) of 1,129,113 bbl. $N_{Z(R2)}$ has a drainage area estimated at 177 acres for OIP and 112 acres for gas in place (GIP) with corresponding OIP of 14,711,551 bbl and GIP of 25,291,285 cu.ft., and V_{RO} of 4,780,666 bbl and the associated recoverable gas volume (V_{Rg}) of 1,797,986,922 cu.ft. In the same vein, $N_{Z(R3)}$ drainage area is 152 acres, having OIP estimated at 28,206,847 bbl with the corresponding V_{RO} of 6,661,986 bbl.

Evaluations based on petrophysical and seismic models [11,12,45–50] have proven resourceful in achieving related objectives in oil and gas fields worldwide and within the Niger Delta. Quantitative and qualitative reservoir evaluations involving seismic and petrophysics-based attributes are essential in reserve estimation. Therefore, as presented by this report, a detailed study involving didactic images and avoiding exaggerating or underestimating the input parameters is dependable as a decision-making tool for planning production activities. However, reservoir estimations involving seismic and petrophysical models with the associated equations come with uncertainties. Regardless, they have been in use, recording successes for hydrocarbon exploration and production projects. Nonetheless, to reduce the related risks involving computational errors, this work engaged repeated readings and calculations, and multiple values recorded are averaged for the desired parameters

6. Conclusions

Reservoirs $N_{Z(R1)}$, $N_{Z(R2)}$ and $N_{Z(R3)}$, delineated across wells $N_{Z(W1)}$, $N_{Z(W2)}$ and $N_{Z(W3)}$, were engaged to characterise the sandstone units and predict the hydrocarbon producibility in N_Z Oil and Gas Field, Offshore Niger Delta. The results show that the field has considerable hydrocarbon reserves. The study indicates sites for viable production wells on the north-eastern and south-eastern axis of the study area to capture hydrocarbons in a possible commercial quantity at the fault-assisted closures. The availability of significant gas quantity at a depth below 10,500 ft at the central portion of the field makes it suitable for exploitation. The central part of the field had structural highs (anticlines) sandwiched between the growth faults, capable of harbouring hydrocarbons. The analysis of the wireline logs revealed almost shale free and porous sandstone units with estimated commercially favourable reserves. The values obtained for free fluid index (FFI) and permeability (k) represent a field with significant transmissibility, indicating a considerable moveable hydrocarbon volume; therefore, there should be reasonable rates of primary hydrocarbon recoveries from the reservoirs. The total recoverable volume of oil (V_{RO}) (11.3×10^6) and gas (V_{Rg}) of (1.8×10^9 cu.ft.) across the study location are significant. The study ensures seismic inputs, porosity, and the dependent parameters are not exaggerated or underestimated, reducing the associated uncertainties.

Future work should include 4D data and possibly, core samples for detailed study to improve the seismic interpretation and compare the results obtained based on the wireline logs.

CRedit authorship contribution statement

Anthony I Nzekwu: Conceptualisation, Investigation, Formal analysis, Writing—original draft.
Richardson M Abraham-A: Conceptualisation, Investigation, Formal analysis, Writing—original draft.

Acknowledgement

Sincere appreciation goes to God for life and inspiration. Thanks to Chevron Nigeria Limited for the software (Kingdom Suite) and data provided during the evaluation.

Conflict of interest

The authors declare no conflict of interest.

References

1. Ofoma AE, Otoghile C, Okogbu CO, et al. (2008) Petrophysical Evaluation of Reservoirs. Examples from Exploratory Oil Wells drilled in the Anambra Basin, South Eastern Nigeria. *Niger Asso Pet Explorationists Bull* 20: 72–80.
2. Rotimi JO, Ameloko AA, Adeoye TO (2009) Applications of 3-D Structural Interpretation and Attribute Seismic Analysis to Hydrocarbon Prospecting over “X” Field Niger Delta. *Int J Basic Appl Sci* 10: 28–40. Available from: www.ijens.org/105104-8383/IJBAS-IJENS.pdf
3. Abraham A (2014) Delineation of a Productive Zone in “Abjnr” Oil Field, Southwestern Niger Delta. *IJES* 3: 31–37. Available from: <http://www.theijes.com/papers/v3-i1/Version-2/E030102031037.pdf>
4. Okwoli E, Obiora D, Adewoye O, et al. (2015) Reservoir characterisation and volumetric analysis of “Lona” field, Niger Delta, using 3-D seismic and well log data. *Pet Coal* 57: 108–119. Available from: http://www.vurup.sk/wp-content/uploads/dlm_uploads/2017/07/pc_2_2015_okwoli_315_v2.pdf
5. Oyeyemi KD, Aizebeokahi AP (2015) Hydrocarbon trapping mechanism and petrophysical analysis of Afam field, offshore Nigeria. *Int J Phys Sci* 10: 222–238. <https://doi.org/10.5897/IJPS2015.4275>
6. Adagunodo AT, Sunmonu AL, Adabanija AM (2017) Reservoir characterisation and seal integrity of Jemir field in Niger Delta, Nigeria. *J Afr Earth Sci* 129: 779–791. <https://doi.org/10.1016/j.jafrearsci.2017.02.015>
7. Abraham-A MR, Taioli F (2020) Asserting the pertinence of the interdependence of seismic images and wireline logs in evaluating selected reservoirs in the Osland field, offshore Niger Delta, Nigeria. *Heliyon* 6: 1–9. <https://doi.org/10.1016/j.heliyon.2020.e05320>
8. Abraham-A MR, Tassinari CCG (2021) CO₂ storage algorithms involving the hybrid geological reservoir of the Irati Formation, Parana Basin. *Int J Greenhouse Gas Control* 112: 103504. <https://doi.org/10.1016/j.ijggc.2021.103504>

9. Keary P, Brooks M (1991) *Introduction to Geophysical Exploration*, Blackwell Scientific Publication, Oxford, 44–47.
10. Abraham-A MR, Taioli F (2017) Maximising Porosity for Flow Units Evaluation in Sandstone Hydrocarbon Reservoirs. Case Study of Ritchie’s Block, Offshore Niger Delta. *J Appl Geol Geophys* 3: 6–16.
11. Abraham-A MR, Taioli F (2019) Hydrocarbon viability prediction of some selected reservoirs in Osland Oil and gas field, Offshore Niger Delta, Nigeria. *Mar Pet Geol* 100: 195–203. <https://doi.org/10.1016/j.marpetgeo.2018.11.007>
12. Oluwadare OA, Olowokere MT, Taoili F, et al. (2020) Application of time-frequency decomposition and seismic attributes for stratigraphic interpretation of thin reservoirs in “Jude Field”, Offshore Niger Delta. *AIMS Geosci* 6: 378–396. <https://doi.org/10.3934/geosci.2020021>
13. Wang Q (1995) Reservoir Delineation using 3-D Seismic Data of the Ping Hu Field, East China. Thesis, University of Colorado.
14. Lines RL, Newrick RT (2004) *Fundamentals of Geophysical Interpretation*. Society of Exploration Geophysicists, 7–9.
15. Asquith G, Krygowski D (2004) Relationships of Well Log Interpretation in Basic Well Log Analysis Methods in Exploration Series. *Am Assoc Pet Geol Bull* 16: 140. <https://doi.org/10.1306/Mth16823>
16. Adeoye TO, Enikanselu PA (2009) Hydrocarbon Reservoir Mapping and Volumetric Analysis Using Seismic and Borehole Data over “Extreme” Field, Southwestern Niger Delta. *Ozean J Appl Sci* 2: 429, 440.
17. Abraham-A MR, Taioli F (2018) Redefining fluids relative permeability for reservoir sands. (Osland oil and gas field, offshore Niger Delta, Nigeria). *J Afr Earth Sci* 142: 218–225. <https://doi.org/10.1016/J.JAFREARSCI.2017.10.024>
18. Byrnes T (2002) Definitions and Guidelines for Estimating and Classifying Oil and Gas Reserves. *Canadian Institute of Mining, Metallurgy and Petroleum Standing Committee on Reserves Definitions* 51: 1–10.
19. Mustafa VK, Egemen K, Serhat A (2006) Estimation of Expected Monetary Values of Selected Oil Fields. *J Econ Plann Policy* 1: 213–221. <https://doi.org/10.1080/15567240500400788>
20. Anstey NA, Geyer RL (1990) Borehole Velocity Measurements and the Synthetic Seismogram. *IHDRC Man*, 197–207.
21. Stacher P (1995) *Present understanding of the Niger Delta hydrocarbon habitat*, Geology of Deltas: Rotterdam, 257–267.
22. Short KC, Stauble AJ (1967) Outline of Geology of Niger Delta. *Am Assoc Pet Geol Bull* 51: 761–779. <https://doi.org/10.1306/5D25C0CF-16C1-11D7-8645000102C1865D>
23. Frankl EJ, Cordry EA (1967) The Niger Delta Oil Province: Recent Developments On-Shore and Off-Shore. *7th World Pet Congr*, 195–209.
24. Doust H, Omatsola E (1989) Niger Delta, *Divergent/Passive Margin Basins*, American Association of Petroleum Geologists, 239–248. <https://doi.org/10.1306/M48508C4>
25. Evamy BD, Haremboure J, Kamerling P, et al. (1978) Hydrocarbon Habitat of Tertiary Niger Delta. *Am Assoc Pet Geol Bull* 62: 1–39. <https://doi.org/10.1306/C1EA47ED-16C9-11D7-8645000102C1865D>
26. Rieijers TJA, Petters SW, Nwajide CS (1997) The Niger Delta Basin. *Sediment Basins World* 3: 151–172. [https://doi.org/10.1016/S1874-5997\(97\)80010-X](https://doi.org/10.1016/S1874-5997(97)80010-X)

27. Ekweozor CM, Okoye NV (1980) Petroleum Source Bed Evaluation of Tertiary Niger Delta1: GEOLOGIC NOTES. *Am Assoc Pet Geol Bull* 64: 1251–1259. <https://doi.org/10.1306/2F919472-16CE-11D7-8645000102C1865D>
28. Weber KJ (1971) Sedimentological Aspects of Oil Fields in the Niger Delta. *Geol Mijnbouw* 50: 559–576.
29. Lambert-Aikhionbare DO, Ibe AC (1984) Petroleum Source Bed Evaluation of Tertiary Niger Delta: Discussion1. *Am Assoc Pet Geol Bull* 68: 387–389. <https://doi.org/10.1306/AD460A2B-16F7-11D7-8645000102C1865D>
30. Nwachukwu JI, Chukwurah PI (1986) Organic Matter of Agbada Formation Niger Delta. *Am Assoc Pet Geol Bull* 71: 48–55.
31. Opara AI, Onuoha KM, Anowai C, et al. (2008) Overpressure and trap integrity studies in parts of the Niger Delta Basin: implication for hydrocarbon prospectivity. *Niger Assoc Pet Explo* 20: 24–30.
32. Magbagbeola OA, Willis BJ (2007) Sequence stratigraphy and syndepositional deformation of the Agbada Formation, Robertkiri field, Niger Delta, Nigeria. *Am Assoc Pet Geol Bull* 91: 945–958. <https://doi.org/10.1306/02050705150>
33. Weber KJ, Daukoru EM (1975) Petroleum Geology of the Niger Delta, *Proceedings of the Ninth World Petroleum Congress*, Applied Science Publishers, 210–221.
34. Genik GJ (1993) Petroleum Geology of the Cretaceous-Tertiary rifts basins in Niger, Chad and the Central African Republic. *Am Assoc Pet Geol Bull* 77: 1405–1434. <https://doi.org/10.1306/BDF8EAC-1718-11D7-8645000102C1865D>
35. Stacher P (1995) *Present understanding of the Niger Delta hydrocarbon habitat*, Geology of Deltas: Rotterdam, 257–267.
36. Freddy C, John HS, Frank B (2005) Structural styles in the deep-water Fold and Thrust Belts of the Niger Delta. *Am Assoc Pet Geol Bull* 89: 753–780. <https://doi.org/10.1306/02170504074>
37. Jolly BA, Lidia L, Whittaker AC (2016) Growth history of fault-related folds and interaction with seabed channels in the toe-thrust region of the deep-water Niger delta. *Mar Petrol Geol* 70: 58–76. <https://doi.org/10.1016/j.marpetgeo.2015.11.003>
38. Lehner P, De Ruiter PAC (1977) Structural history of Atlantic Margin of Africa. *Am Assoc Pet Geol Bull* 61: 961–981. <https://doi.org/10.1306/C1EA43B0-16C9-11D7-8645000102C1865D>
39. Tuttle MT, Charoentier RR, Brownfield ME (1999) The Niger Delta Petroleum System: Niger Delta Province, Nigeria, Cameroon, and Equatorial Guinea, Africa. *US Geol Surv*, 1–44. <https://doi.org/10.3133/ofr9950H>
40. Rowan MG, Peel FJ, Vendeville (2004) Gravity-driven fold belts on passive margins. *AAPG Mem* 82: 157–182. <https://doi.org/10.1306/61EECE28-173E-11D7-8645000102C1865D>
41. Brownfield ME, Charpentier RR (2006) Geology and Total Petroleum Systems of the WestCentral Coastal Province (7203), West Africa. *US Geol Surv Bull*. <https://doi.org/10.3133/b2207B>
42. Schlumberger (1989) Permeability and Productivity; Log Interpretation Principles and Application. Schlumberger Education Services, Houston, 10–11 to 10–14.
43. Coates G, Denoo S (1981) The producibility answer product. *Tech Rev* 29: 55–66.
44. Bateman R, Fessler H (1986) *Openhole log analysis and formation evaluation*, United States, 8.1–8.3.

45. Hamed EM, Kurt JM (2008) Structural interpretation of the Middle Frio Formation using 3-D seismic and well logs: an example from the Texas Gulf Coast of the United States. *Leading Edge* 27: 840–854. <https://doi.org/10.1190/1.2954023>
46. Ishwar NB, Bhardwaj (2013) A Petrophysical Well Log Analysis for Hydrocarbon exploration in parts of Assam Arakan Basin, India. 10th Biennial International Conference Exposition.
47. Abraham-A R (2013) Well Correlation and Petrophysical Analysis, a Case Study of “Rickie” Field Onshore Niger Delta. *Int J Eng Sci* 2: 94–99.
48. Pigott JD, Kang MH, Han HC (2013) First Order Seismic Attributes for clastic Seismic facies Interpretation: Examples from the East China Sea. *J Asian Earth Sci* 66: 34–54. <https://doi.org/10.1016/j.jseaes.2012.11.043>
49. Goodway B, Perez M, Varsek J, et al. (2010) Seismic petrophysics and isotropic-anisotropic AVO methods for unconventional gas exploration. *Leading Edge* 29: 1433–1544. <http://dx.doi.org/10.1190/1.3525367>
50. Holdaway KR, Irving HBD (2017) *Enhance Oil & Gas Exploration with Data-Driven Geophysical and Petrophysical Models*. <https://doi.org/10.1002/9781119394228>



AIMS Press

© 2022 the Author(s), licensee AIMS Press. This is an open-access article distributed under the terms of the Creative Commons Attribution License (<http://creativecommons.org/licenses/by/4.0>)